THE JOURNAL OF PHYSICAL CHEMISTRY C

Article

pubs.acs.org/JPCC

Hydrogen Recombination Rates on Silica from Atomic-Scale Calculations

Kyle K. Mackay, Jonathan B. Freund, and Harley T. Johnson*

Department of Mechanical Science and Engineering, University of Illinois at Urbana−Champaign, Urbana, Illinois 61801, United States

ABSTRACT: A combined molecular dynamics (MD) and Monte Carlo approach was used to bridge time scales, enabling calculations of surface recombination rates for hydrogen on silica. MD was used for temperatures between 10 and 600 K at a high pressure of 10 atm, yielding recombination coefficients between 0.1 and 1. For the lower pressures more common in applications, low recombination rates make the corresponding calculations intractably expensive. A Monte Carlo technique, informed by the MD simulations, was designed to bridge the essential time scales. Distinct weak and strong surface binding sites for atomic hydrogen with densities of approximately 10 nm^{-2} were found using grand canonical Monte Carlo (GCMC) simulations, which, in turn, were used to obtain Eley−Rideal rate constants based on semiequilibrium theory. Monte Carlo variational transition state theory (MCVTST) was used to calculate Langmuir−Hinshelwood and thermal desorption rate constants for hydrogen atoms in strong and weak adsorption sites. Calculated reaction rates were used in a Langmuir kinetics model to estimate the recombination coefficient γ for T = 10−2000 K at gas-phase radical densities between 10^{12} and 10^{16} cm^{-3}, yielding values of $\gamma = 10^{-4}$−0.9.

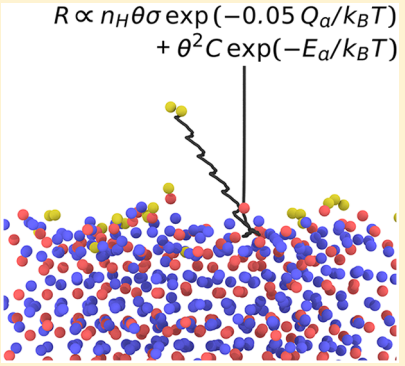

1. INTRODUCTION

1.1. Hydrogen Recombination on Silica. The recombination of hydrogen on surfaces can be a key factor in the production of molecular hydrogen in the interstellar medium[1−4] and in controlled fusion devices[5−7] and for the storage of hydrogen in low-density carbon nanostructures.[8,9] This elementary reaction must be taken into consideration for many modern engineering applications.

Because it is abundant and relatively inert, silica is a common surface considered in experimental and theoretical studies on surface-mediated hydrogen recombination. Recombination of hydrogen on glass surfaces is thought in some cases to serve as a source of contamination in vacuum experiments, obscuring the phenomena being studied and destroying radicals unless suitable precautions are taken.[10−12]

Quartz and other silica derivatives are likewise commonly chosen materials for surfaces intended to be chemically inert. However, reported reactivities of silica vary widely, with its surface catalycity reported to be on a par with that of platinum for high temperatures.[13] The lack of a surface chemistry model for silica prevents a quantitative prediction of the influence these materials have on bulk chemistry.[14,15] This is particularly important in combustion applications on the micrometer scale, where the high surface-to-volume ratio exaggerates the relative importance of radical quenching at the walls.[16,17]

1.2. Background: Experiments and Models. Langmuir first observed that hydrogen radicals are strongly bound to glass surfaces, proposing that these adatoms form a tightly packed monolayer on the silica surface.[18,19] It was later shown that, although hydrogen is adsorbed, it is not closely packed.[20] Subsequent studies suggested two main bound states, one weak and one strong, that exist in approximately equal densities. Although their energies are known to be different, their specific values have been hard to quantify, with values ranging from 25 to 45 kcal/mol for the strongly bound state and from 1.5 to 4 kcal/mol for the weakly bound state.[10,21−25] Although some of the proposed models for hydrogen−quartz interactions can be applied to surfaces with micro- and nanometer-scale roughness, they are unable to account for atomic-scale variations in the surface. These variations provide pits and crevasses that can significantly increase the strength of H-atom adsorption, resulting in the measured bond energy being larger than model predictions by a factor of 4.[21]

Most of the experimental studies of hydrogen recombination on silica have been based on the axial decay of the radical number density in a silica tube. Radicals are generated near the inlet by a plasma discharge, diffusing to the walls and down the length of the tube. The corresponding models take a uniform radical number density at the inlet and assume that radicals recombine at the walls at a constant rate due to recombination. The estimated recombination rates are sensitive to chosen boundary conditions for the diffusion problem and the anticipated effect of the invasive method used to measure the radical number density. Studies of this reaction have made a number of assumptions in the analysis of experimental data. Some models have been based on low ($\theta \approx 0$) or high ($\theta \approx 1$) surface coverage, whereas others assert that either Langmuir−Hinshelwood or Eiley−Rideal recombination dominates the

Received: July 22, 2016
Revised: September 19, 2016
Published: October 5, 2016

DOI: 10.1021/acs.jpcc.6b07365
J. Phys. Chem. C 2016, 120, 24137−24147

production of molecular hydrogen.[21,26] Figure 1 summarizes large disparities in the experimental data and the model

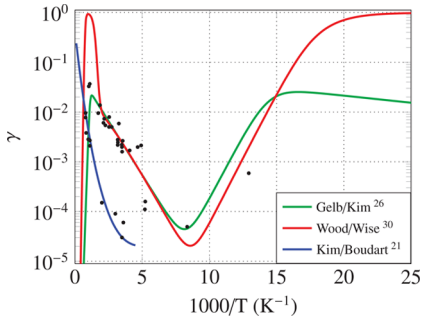

Figure 1. Summary of models (solid lines) and measurements (scatter points) for the recombination coefficient of hydrogen on silica.[31]

predictions. By representing reactions at the atomic scale, we intend to circumvent many of the assumptions made in experimental studies by directly measuring activation energies and reaction rates.

1.3. Simulation-Integrated Modeling Approach. Molecular dynamics (MD) simulations are attractive for the study of nanometer- to micrometer-scale dynamics; however, only short time scales ($\lesssim 10^{-9}$ s) can be directly simulated. As a result, direct MD simulation is restricted to unrealistically high partial pressures for radical species so that enough radical−surface interactions can be observed to converge meaningful statistics.[27,28] More recently, semiclassical dynamics calculations with quantized lattice vibrations and classically modeled gas particles have been used to estimate the recombination coefficient of hydrogen on crystalline quartz.[29] However, even these simulations were fundamentally limited to small time and length scales as a result of the need to accurately simulate the time dynamics of the system.

The goal of this study is to develop a method to bridge these challenging time-scale disparities while retaining the detail afforded by atomic-scale calculations. For our model, we consider four types of surface reactions. The first is the Eley−Rideal (ER) recombination mechanism, where a gas-phase hydrogen atom directly impinges on an adsorbed hydrogen atom and recombines

$$H(g) + H(s) \xrightarrow{k_{ER}} H_2(g)$$

This reaction is first-order with respect to both gas-phase radical concentration and surface coverage. At high temperatures, adsorbed atoms become mobile on the surface, enabling a second mechanism: Langmuir−Hinshelwood (LH) recombination

$$H(s) + H(s) \xrightarrow{k_{LH}} H_2(g)$$

This reaction is second-order with respect to surface coverage and occurs when two adsorbed hydrogen atoms meet each other as a result of diffusion on the surface. At even higher temperatures, adsorbed hydrogen atoms are ejected from the surface as a result of thermal desorption

$$H(s) \xrightarrow{k_D} H(g)$$

which is first-order with respect to surface coverage. Finally, the adsorption of gas-phase hydrogen radicals on the surface is considered

$$H(g) \xrightarrow{k_A} H(s)$$

This process is first-order with respect to gas-phase radical concentration and populates the surface with hydrogen atoms from the gas phase, enabling surface reactions.

The interatomic potential used in our calculations is described in section 2.1. The model is used to quantify hydrogen recombination rates on a realistic but ideally "clean" amorphous quartz (silica) surface, which is also introduced in section 2.1. In section 2.2, radical−surface interactions are simulated at high pressures with molecular dynamics to measure recombination rates in an extreme high-pressure regime inaccessible to experiments. A Monte Carlo procedure to calculate surface reaction rates using atomic-scale methods is outlined in section 2.3. Section 2.4 addresses the grand canonical Monte Carlo calculations used to measure the densities and binding energies for hydrogen adsorption sites on the silica surface. Reaction rates for Eley−Rideal recombination are estimated using semiequilibrium theory. Section 2.5 covers the Monte Carlo variational transition state theory (MCVTST) calculations used to quantify the rates of the Langmuir−Hinshelwood and thermal desorption reactions. A multi-time-scale Langmuir kinetics model is constructed in section 3.1 using the reaction rates found in the atomic-scale simulations. Finally, recombination rates predicted by this model are compared to molecular dynamics simulations and experimental results in sections 3.1 and 3.2.

2. COMPUTATIONAL METHODS AND RESULTS

2.1. Preliminaries. All molecular dynamics simulations in this work were performed using LAMMPS.[32] The ReaxFF bond-order potential for Si−O−H systems ($ReaxFF_{SiO}$[33]) was used with the parametrization of Si terms for free surfaces found in refs 34 and 35. Parameters relevant for H and O remain unchanged from ref 33.

$ReaxFF_{SiO}$ has been used extensively in studying the interactions of gases,[34] liquids,[36] and acids[37] with crystalline and amorphous silica. Depending on the training set used in parametrization, the potential has been shown to produce interaction energies and bond lengths that are in agreement with quantum calculations and experimental results. In general, ReaxFF reproduces heats of formation to within 2.0 kcal/mol (0.1 eV), bond lengths to within 0.01 Å, and bond angles to within 2° of their literature values, and it has been validated by comparing its predictions with an extensive set of experimental data and quantum chemistry (density functional theory) calculations.[33,38] The current ReaxFF Si−O−H surface was constructed using electronic structure data and validated with experimental data in ref 33, with further refinement for surfaces in ref 35.

A repeated melt−quench procedure was used to produce the amorphous surface used in later calculations. An α-quartz slab consisting of 1575 atoms ($5 \times 7 \times 5$ unit cells) was initialized at a temperature of 300 K. The temperature of the slab was raised to 4000 K at a rate of 25 K/ps under *NVT* dynamics using a Nosé−Hoover thermostat. The silica melt was then cooled back to 300 K at the same rate. The system temperature was raised once again to 4000 K using *NPT* dynamics with a Berendsen barostat, after which it was cooled to 300 K. The latter melt−quench procedure was performed at heating and cooling rates of 25 K/ps at a pressure of 1 atm. This procedure was found to reliably replicate the structural and chemical

DOI: 10.1021/acs.jpcc.6b07365
J. Phys. Chem. C 2016, 120, 24137−24147

properties of amorphous silica using the ReaxFF potential in several past studies.[33,39,40]

2.2. Molecular Dynamics. *2.2.1. Methods.* By directly simulating recombination with molecular dynamics, it is possible to measure reaction rates in regimes outside those commonly explored in experiments, thus providing additional data for the assessment of a multi-time-scale model. MD simulations of the sequential impact of H radicals on a silica surface were performed at several surface temperatures in the range of 10−600 K. In each case, the gas was assumed to be in thermal equilibrium with the surface. A schematic of the simulation cell can be seen in Figure 2. Hydrogen radicals were

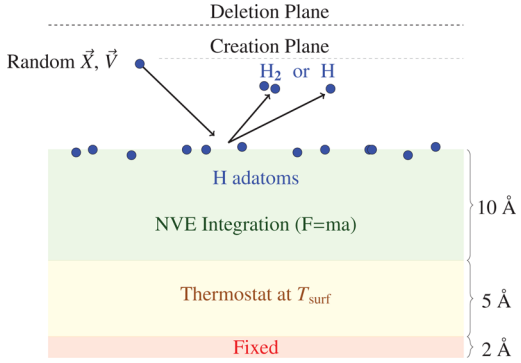

Figure 2. Schematic of the simulation box for MD bombardment simulations.

generated in random positions on a plane 10 Å above the silica surface and given velocities sampled from the Maxwell−Boltzmann distribution. The composition of each molecule crossing a plane 15 Å above the surface was determined, after which the molecule was removed from the simulation. At each temperature, 1500−2000 hydrogen impacts were simulated, and the recombination coefficient was calculated as the fraction of H atoms that left the surface as part of a H_2 molecule

$$\gamma_{H_2} = \frac{2N_{H_2,out}}{2N_{H_2,out} + N_{H,out}} \quad (1)$$

where $N_{i,out}$ is the number of species i that crossed the deletion plane over the course of the MD simulation. The time between each hydrogen−surface impact was

$$\tau = \frac{A}{n_H}\left(\frac{2\pi m_H}{k_B T}\right)^{1/2} \quad (2)$$

where n_H is the number density of hydrogen radicals in the gas phase, m_H is the mass of a hydrogen atom, k_B is the Boltzmann constant, T is the temperature of the gas, and A is the quartz surface area. Unfortunately, the use of classical molecular dynamics simulations restricted us to short time scales. To sample a sufficient number of hydrogen impacts in MD-accessible time scales, we resorted to simulating high partial pressures of the H radical. In these simulations, we chose a gas-phase number density of $n_H = 2.7 \times 10^{20}$ cm^{-3} for the H radical, corresponding to a pressure of approximately 10 atm at 300 K.

2.2.2. Results. For each temperature, the first 100−1000 impacts served the sole purpose of populating the surface with hydrogen atoms. After hydrogen coverage on the surface reached steady state, subsequent hydrogen impacts were used to calculate the recombination coefficient. This process was repeated for $T_{surf} = T_{gas}$ = 10, 20, 50, 100, 200, 275, 350, 400, 500, and 600 K. As encountered in other high-pressure molecular dynamics studies, the recombination coefficient determined in this work is quite high.[28] Because of the extremely high number density of H radicals in the gas phase, recombination is dominated by the Eley−Rideal mechanism, which is first-order with respect to gas-phase number density. This recombination mechanism also has a significantly lower activation energy than the LH mechanism and occurs on a faster time scale. The collected recombination coefficients can be seen in Figure 3. The error bars on the MD data come from

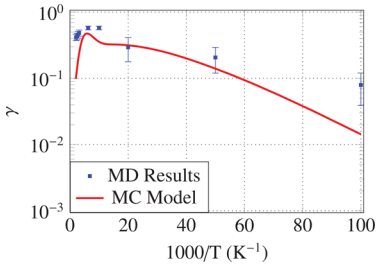

Figure 3. Recombination coefficients measured in MD bombardment simulations (described in section 2.2) and computed using a Langmuir kinetics model (parametrized using the procedure outlined in section 2.3).

the finite number of impacts performed at each temperature. The computed recombination coefficients increase with temperature until 275 K, at which point they begin to decrease with increasing temperature. This is due to the thermal desorption of physisorbed H atoms. As weakly bound H atoms are removed from the surface, the "weakest link" in the recombination process is removed, and incoming H radicals must overcome greater energy barriers to recombine with chemisorbed hydrogen atoms.

2.3. Monte Carlo Procedure. To calculate reaction rates relevant to surface-mediated recombination, we had to overcome the limited time scales of MD simulations. To account for the relevant surface processes (LH recombination, ER recombination, and thermal desorption), we used a two-step Monte Carlo procedure:

(1) The grand canonical Monte Carlo (GCMC) method was used to measure the density of adsorption sites on the silica surface and the heat of adsorption of H radicals in each of these sites. From this information, we estimated an ER reaction rate.
(2) After generating a surface with full hydrogen coverage, Monte Carlo variational transition state theory (MCVTST) was used to calculate the reaction rates for LH recombination and thermal desorption.

2.4. Grand Canonical Monte Carlo Simulations. *2.4.1. Methods.* The grand canonical ensemble, in which the temperature (T), volume (V), and chemical potential (μ) of the system are fixed, provides the appropriate conditions for studying adsorption. After the silica surface is exposed to a reservoir of gas-phase H radicals at a fixed chemical potential, an equilibrium will be reached where the potential energy of H atoms adsorbed on the surface and the chemical potential of radicals in the reservoir are equal, that is

$$\mu[H(s)] = \mu[H(g)]$$

The grand canonical Monte Carlo (GCMC) method is therefore an equilibrium technique for sampling observables

DOI: 10.1021/acs.jpcc.6b07365
J. Phys. Chem. C 2016, 120, 24137−24147

in the μVT ensemble, for example, the average number of particles adsorbed on the surface (or, equivalently, the surface coverage θ) at a prescribed chemical potential μ.

The simulation of adsorption in this ensemble proceeds through three mechanisms:[41−43]

(1) Displacement of a particle: A random particle with position $\mathbf{R}$ is selected and given a random displacement $\delta\mathbf{R}$. This move is accepted with a probability of

$$P(\mathbf{R} \rightarrow \mathbf{R} + \delta\mathbf{R}) = \min(1, \exp\{-\beta[U(\mathbf{R} + \delta\mathbf{R}) - U(\mathbf{R})]\})$$

(2) Insertion of a hydrogen atom: A new particle is inserted at a random position in the volume V. Atom insertion is accepted with a probability of

$$P(N \rightarrow N + 1) = \min\left(1, \frac{V}{\Lambda^3(N+1)} \exp\{\beta[\mu - U(N+1) + U(N)]\}\right)$$

(3) Removal of a hydrogen atom: A random hydrogen atom in volume V is removed. The deletion is accepted with a probability of

$$P(N \rightarrow N - 1) = \min\left(1, \frac{\Lambda^3 N}{V} \exp\{-\beta[\mu + U(N-1) - U(N)]\}\right)$$

In the preceding equations, $\beta = 1/k_B T$ and $\Lambda = (h^2/2\pi m k_B T)^{1/2}$ is the thermal de Broglie wavelength (h is Planck's constant, and m is the particle mass). U is the potential energy of the system, which we calculated using the ReaxFF potential. Because we are interested in low number densities of H radicals, the reservoir potential, μ, was calculated with the Sackur−Tetrode equation for an ideal gas

$$\mu = -k_B T \log\left[\frac{1}{n_H}\left(\frac{2\pi m_H k_B T}{h^2}\right)^{3/2}\right] \quad (3)$$

where n_H is the number density of H radicals in the gas phase and m_H is the mass of a hydrogen atom.

Beginning with the uncontaminated silica surface obtained in section 2.1, one of these three procedures (displacement, insertion, or removal) was attempted during each GCMC step. An acceptance rate of 20% for proposed moves was achieved through a careful choice of the magnitude of atomic displacement and by biasing moves toward atomic displacement or atomic creation/deletion. The acceptance rate for addition and deletion of particles is typically low (about 3% at steady state, compared to 50% for moving a particle). The relatively rare acceptance of particle deletion/creation does more to advance the simulation than particle displacement, however. Deleting a particle in one position and creating another particle in a different position is equivalent to many successive particle displacements. For this reason, proposed moves in the GCMC process were biased toward particle creation and deletion. Steps were repeated until the surface coverage and system potential energy reached steady state.

A reflecting barrier for silicon and oxygen atoms was placed 1 Å above the surface to prevent removal of these atoms from the silica. To prevent the formation of gas-phase H_2, any proposed move that resulted in a chemical bond between H atoms was rejected. Other parameters used in these simulations, including the probability of a proposed move being a particle addition (p_{add}), deletion (p_{del}), or displacement (p_{disp}), are listed in Table 1.

Table 1. Values Used for Various Parameters in GCMC Simulations of H Adsorption on Silica

parameter	value
$\lvert\delta\mathbf{R}\rvert$	0.1 Å
n_H	10^{12} cm^{-3}
p_{disp}	0.2
p_{add}	0.4
p_{del}	0.4

After a surface with full coverage had been obtained, the heat of adsorption for each accessible site was calculated as the difference in system potential energy after the atom occupying the site had been displaced to a location 1 nm above the surface. Increasing this distance had no effect on the calculated heats of adsorption.

2.4.2. Results. The convergence of the system potential energy and hydrogen coverage for T = 750 K can be seen in Figure 4. High-temperature cases with low surface coverage typically reach steady state within (1−2) × 10^6 moves, whereas low-temperature simulations with high surface coverage converge at only half that rate.

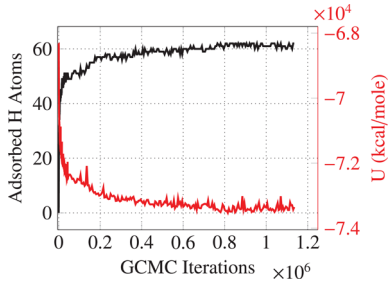

Figure 4. Number of adsorbed H atoms and system potential energy as a function of GCMC steps for T = 750 K.

As can be seen in Figure 5, the density of accessible surface sites at high temperatures (1000 > T > 70 K) remains relatively constant at 9.3 nm^{-2}, resulting in a surface similar to the one seen in Figure 6. Hydrogen adatoms are tightly bound to the surface, sitting in atomic-scale pits and forming bonds with previously undercoordinated surface atoms. These surface defects, primarily undercoordinated silicon and nonbridging oxygen atoms, play a critical role in heterogeneous recombi-

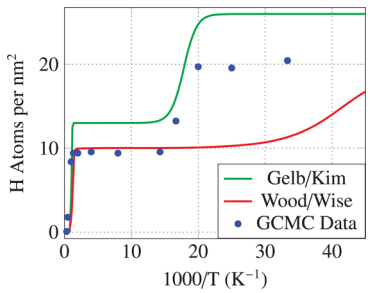

Figure 5. Density of adsorbed H atoms as a function of temperature from GCMC results. Surface coverage predicted by surface chemistry models found in refs 26 and 30 are shown for comparison.

DOI: 10.1021/acs.jpcc.6b07365
J. Phys. Chem. C 2016, 120, 24137−24147

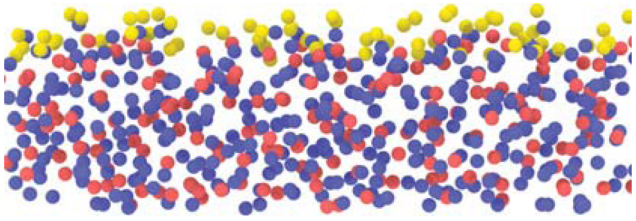

Figure 6. Cross section of a silica surface with fully occupied strong adsorption sites (θ_S = 1).

nation. In addition to serving as adsorption sites, they lower the barrier of reactions, catalyzing recombination on the silica surface. The effect of individual silica defects on oxygen recombination has been explored in detail using electronic structure calculations.[44] Although the effects of specific defects were not explored here, defects are expected to contribute similarly to hydrogen recombination.

The distribution of heats of adsorption for these strong surface sites can be seen in Figure 7. The peak centered at 40

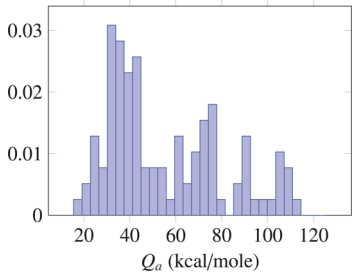

Figure 7. Distribution of heats of adsorption for strong adsorption sites from grand canonical Monte Carlo simulations.

kcal/mol mostly consists of hydrogen atoms in silanol (Si−O−H) groups on the surface, whereas higher heats of adsorption correspond to Si−H bonds and adsorption sites in pits on the surface. The density of chemisorption sites on the surface is similar to the measured values of 10−13.5 nm^{-2}.[45,46] The density of hydroxyl groups on the surface, defined as hydrogen atoms with a bond order of 0.9 or greater with a surface oxygen atom, is 4.2 nm^{-2}. This value is in agreement with the density measured by Zhuravlev (4.5 nm^{-2}).[47]

After the temperature is reduced below 70 K, the chemical potential of the H reservoir increases to the point that physisorption sites become accessible to gas-phase radicals. The number of adsorbed hydrogen atoms approximately doubles, and the surface depicted in Figure 8 is obtained. GCMC calculations predict a physisorption site density of 10.5 nm^{-2}. Because of the finite size of the simulated surface, an error of ±1 adsorption site is assumed, which translates into an error in surface site density of ±0.15 nm^{-2}.

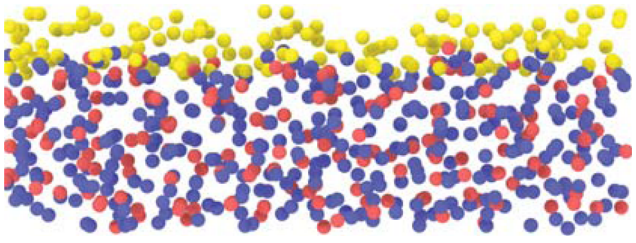

Figure 8. Cross section of a silica surface with fully occupied strong and weak adsorption sites ($\theta_S = \theta_W$ = 1).

Because of the double-plateau behavior seen in Figure 5, we adopted the "strong" and "weak" surface coverage model used in previous studies. Strong surface coverage, θ_S, corresponds to hydrogen atoms occupying chemisorption sites, whereas weak surface coverage, θ_W, refers to hydrogen radicals occupying physisorption sites on the surface.

2.4.3. Eley−Rideal Rate Constant. The GCMC calculations provide atomic-level information about active sites and surface coverage, particularly total number of occupied active sites and their respective heats of adsorption. According to semi-equilibrium theory, the probability of a gas-phase radical recombining with an atom in adsorption site j is equal to the probability of the gas atom directly impinging on the occupied active site multiplied by the probability of the gas atom having enough kinetic energy to overcome the reaction barrier

$$\gamma_j = 2gN_j\sigma_{0j}\exp(-E_{a,j}/k_BT) \tag{4}$$

where g is a statistical factor to account for electronic degeneracies and is equal to 0.25 for H_2.[26] N_j is the density of sites of type j per unit area, σ_{0j} is the collisional cross section of an active site of type j, and $E_{a,j}$ is the activation energy of ER recombination for an active site of type j. If we treat each adsorption site on the surface as unique, the ER recombination coefficient for full surface coverage can be calculated as a sum over all active sites found in our GCMC calculations

$$\gamma_{ER} = A^{-1}\sum_{j=1}^{n_{sites}} 2g\sigma_{0j}\exp(-\beta E_{a,j}) \tag{5}$$

$$R_{ER} = k_A\gamma_{ER} \tag{6}$$

where A is the area of the silica surface in our GCMC simulations and k_A is the rate at which gas-phase hydrogen radicals impinge on the silica surface. The collisional cross section of an adsorbed hydrogen atom is approximated as a circle with a radius equal to the H_2 bond length (0.741 Å), or

$$\sigma_{0j} = \pi r_{H_2}{}^2 = 1.72 \times 10^{-16}\ cm^2$$

and the activation energy of the ER reaction is estimated using the Hirschfelder relation for heterogeneous recombination, $E_{a,j} = 0.055Q_{a,j}$, where $Q_{a,j}$ is the heat of adsorption of a hydrogen atom in site j.

2.5. Monte Carlo Variational Transition State Theory. Transition state theory (TST) estimates reaction rates of elementary chemical reactions by assuming a state of quasiequilibrium between reactants and activated transition state complexes. In using Monte Carlo variational transition state theory (MCVTST), one integrates over the contribution of each active site to find the total reaction rates for the chemically active surface, in this case obtaining Langmuir−Hinshelwood and thermal desorption rates for hydrogen atoms on the silica surface.

In the past, this method has been used to calculate rate coefficients for various reactions such as the recombination and desorption rates of H atoms on a pristine Si surface,[48,49] self-diffusion on metal surfaces,[50] and dissociation of complex molecules.[51]

Using transition state theory, we calculated reaction rates for Langmuir−Hinshelwood recombination and thermal desorp-

DOI: 10.1021/acs.jpcc.6b07365
J. Phys. Chem. C 2016, 120, 24137−24147

tion. Figure 9 shows a reaction diagram showing relevant "transition states" for the LH recombination of hydrogen.

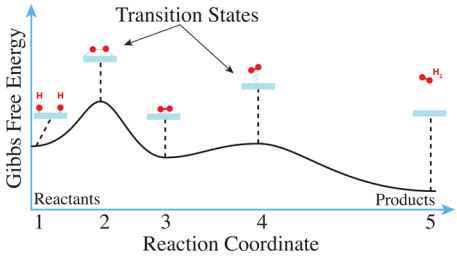

Figure 9. Reaction diagram for Langmuir–Hinshelwood recombination. States include (1) a pair of adsorbed hydrogen atoms, (3) a physisorbed hydrogen molecule, and (5) a desorbed hydrogen molecule. States 2 and 4 are transition states between these equilibrium configurations.

2.5.1. Methods. Given a surface with two adsorbed hydrogen atoms, the TST rate coefficient for the recombination/desorption of H_2 is calculated in terms of the flux across a dividing surface S. This flux is found by integrating over the momentum ($\mathbf{P}$) and position ($\mathbf{R}$) space of atoms in the system

$$k_{LH} = \frac{\int d\mathbf{P} \int d\mathbf{R} \delta_{H_2}(\mathbf{R}_p - \mathbf{R}_s)|V_s| \exp(-\beta H)}{n_s \int d\mathbf{P} \int d\mathbf{R} \exp(-\beta H)} \quad (7)$$

where V_s is the velocity normal to the surface $\mathbf{S}$, $\beta = (k_B T)^{-1}$, n_s is the density of adsorption sites on the surface, and $\delta(\mathbf{R}_p - \mathbf{R}_s)$ is the Dirac delta function with $\mathbf{R}_s$ denoting the location of the dividing surface and $\mathbf{R}_p$ denoting the location of the reaction product. The canonical ensemble average can be evaluated using Monte Carlo sampling, meaning that the integrals in eq 7 can be replaced by the following sum over N states[52,53]

$$k_{LH} = \lim_{N\to\infty} [(Nn_s)^{-1} \sum_{i=1}^{N} \delta_{H_2}(\mathbf{R}_p - \mathbf{R}_s)_i |V_s|_i] \quad (8)$$

The Dirac function is modeled by a narrow Gaussian of the form

$$\delta_{H_2}(\mathbf{R}_p - \mathbf{R}_s) = \frac{1}{\sqrt{2\pi}\omega} \exp[-(z_{cm} - z_s)^2/2\omega^2] \quad (9)$$

where z_{cm} is the center-of-mass height of a H_2 molecule above the surface and z_s is the height of the dividing plane above the surface. ω is assigned a value of 0.275 Å for our calculations and $V_s = \dot{z}_{cm}$.

Similarly, the rate of thermal desorption of hydrogen atoms from the surface can be calculated as

$$k_d = \frac{0.5 \int d\mathbf{P} \int d\mathbf{R}\, \delta_H(\mathbf{R}_p - \mathbf{R}_s)|V_s| \exp(-\beta H)}{\int d\mathbf{P} \int d\mathbf{R} \exp(-\beta H)} = \lim_{N\to\infty} [(2N)^{-1} \sum_{i=1}^{N} \delta_H(\mathbf{R}_p - \mathbf{R}_s)_i |V_s|_i] \quad (10)$$

Here, the delta function of position, $\delta_H(\mathbf{R}_p - \mathbf{R}_s)$, and the velocity normal to the dividing surface, $|V_s|$, use the position and velocity of the H radical nearest the dividing surface.

The convergence of the Monte Carlo sum can be accelerated with importance sampling. With an "expected distribution" function of

$$P^0 = \exp[-\beta(U_{g-s} + U_{g-g})] \quad (11)$$

where U_{g-s} is the potential energy due to gas–surface interactions and U_{g-g} is the potential energy of bonds between gas atoms, we restrict states with high kinetic energies or excessive deviations of lattice atoms from their equilibrium positions. The reaction rates are calculated as

$$k_D = \frac{\sum_{i=1}^{N} \delta_H(\mathbf{R}_p - \mathbf{R}_s)_i |V_s|_i P_i^0}{2 \sum_{i=1}^{N} P_i^0} \quad (12)$$

$$k_{LH} = \frac{\sum_{i=1}^{N} \delta_{H_2}(\mathbf{R}_p - \mathbf{R}_s)_i |V_s|_i P_i^0}{n_s \sum_{i=1}^{N} P_i^0} \quad (13)$$

With this choice, a proposed system state is accepted with a probability of

$$P_{accept} = \exp[\beta(H'_{old} - H'_{new})] \quad (14)$$

where

$$H' = \sum_{i}^{N_s} \frac{1}{2m_i} \mathbf{P}_i \cdot \mathbf{P}_i + \sum_{j}^{N_g} \frac{1}{2m_j} \mathbf{P}_j \cdot \mathbf{P}_j + U_{s-s} \quad (15)$$

U_{s-s} denotes the potential energy from bonds between surface atoms, N_s is the number of atoms in the silica surface, and N_g is the number of gas atoms.[54] In each proposed move, selected surface atoms and gas atoms have their positions and velocities varied by random vectors $\mathbf{dx}$ and $\mathbf{dv}$, respectively. The acceptance rate of moves can be modified by varying the fraction of atoms subject to these displacements during each step and by changing the magnitudes of $\mathbf{dx}$ and $\mathbf{dv}$. After enough states have been sampled, the sum for k_{LH} converges.

To quantify LH recombination for strongly bound H atoms, we prepared a silica surface with an exposed area of 3.5 nm^2 by the melt–quench procedure outlined in section 2.1 and populated it with two hydrogen adatoms (the "gas" atoms). For reactions of weakly bound hydrogen atoms, we prepared the same silica surface and occupied it with H atoms by performing a GCMC simulation with T = 750 K and $n_H = 1 \times 10^{12}$ cm^{-3} until the number of adsorbed H atoms and the system potential energy reached steady state. After all of the chemisorption sites had been occupied, two additional hydrogen atoms were added above the fully covered silica surface. In the latter case, chemisorbed hydrogen atoms were considered to be "surface" atoms, whereas the two physisorbed hydrogen atoms were considered to be gas atoms.

In each case, the dividing plane was located 9 Å above the surface. For every proposed step in the Markov chain, the two gas-phase hydrogen atoms and two surface atoms were selected to have their positions and velocities modified. Each selected atom was displaced by the vector

$$\mathbf{dx} = \delta x(\xi_1 \mathbf{i} + \xi_2 \mathbf{j} + \xi_3 \mathbf{k})$$

and had its velocity changed by the amount

$$\mathbf{dv} = \delta v(\xi_4 \mathbf{i} + \xi_5 \mathbf{j} + \xi_6 \mathbf{k})$$

where ξ_i represents random numbers from a uniform distribution $U(-1,1)$. In our simulations, the magnitudes of these vectors were chosen to be

$$\delta x = 0.05 \text{ Å} \qquad \delta v = 0.05 v_{rms}$$

DOI: 10.1021/acs.jpcc.6b07365
J. Phys. Chem. C 2016, 120, 24137–24147

where v_{rms} is the root-mean-square velocity of an atom of mass m at temperature T

$$v_{rms} = \left(\frac{3k_B T}{m}\right)^{1/2}$$

A reflecting barrier for gas particles was placed at a depth of 1.5 Å beneath the surface to prevent penetration of H and H_2 into the bulk material. Surface atoms at depths greater than 2.5 Å did not have their positions and velocities altered. For H_2 desorption, z_{H_2} and $\dot{z}_{H_2}$ were taken to be the center-of-mass Z position and velocity, respectively, of the gas-phase H_2 molecule. For recombination/desorption on a clean silica surface, rate coefficients were calculated for temperatures between 100 and 2000 K. For a surface with fully occupied strong surface sites, these reaction rates were calculated between 10 and 250 K.

2.5.2. Results. The rates of H_2 and H desorption for full surface coverage, defined as

$$R_{LH} = n_s^2 k_{LH} \qquad R_D = n_s k_D$$

are presented in Figures 10−12. For MCVTST calculations, $(1-4) \times 10^7$ moves were performed in each Markov random

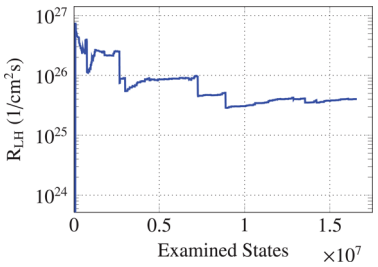

Figure 10. Convergence of the Langmuir−Hinshelwood rate constant over a surface with full hydrogen coverage at T = 250 K.

walk. The convergence of the LH rate constant in one such random walk is shown in Figure 10. To estimate an uncertainty in each obtained rate coefficient, the standard deviation of k_{LH} during the last 8×10^6 moves was measured. In each case, the magnitude of the uncertainty was approximately 10% of the calculated rate constant. The distribution of TST reaction rates can be seen in Figures 11 and 12 for hydrogen atoms in strong and weak adsorption sites, respectively. In each case, the rate constants follow a linear trend in the Arrhenius plot. The slope of the atomic desorption rate constants is greater than that of the molecular desorption rate constants, indicating a higher activation energy for the thermal desorption of hydrogen atoms. Despite the higher activation energy, atomic desorption

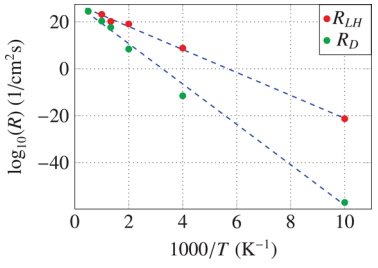

Figure 11. Calculated Langmuir−Hinshelwood and thermal desorption reaction rates for strongly bound hydrogen coverage.

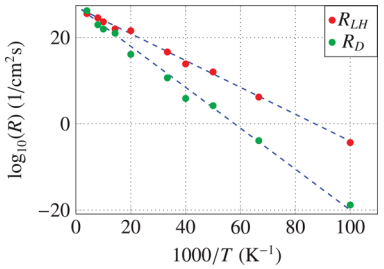

Figure 12. Calculated Langmuir−Hinshelwood and thermal desorption reaction rates for weakly bound hydrogen coverage.

appears to be the dominant process at high temperatures. At this extreme, mobile hydrogen adatoms are capable of overcoming the barrier for desorption without needing to first find another mobile hydrogen atom (a rate-limiting step for LH recombination).

2.5.3. Kinetic Rate Model. By performing a least-squares fit of the Arrhenius equation

$$R(C, E_a, T) = Ce^{-E_a/k_B T} \quad [1/(\text{cm}^2\,\text{s})] \tag{16}$$

to the calculated Langmuir−Hinshelwood and thermal desorption rate constants and accounting for the uncertainty in each measurement, we found the effective activation energies E_a and pre-exponential factors C for these processes. The likelihood of E_a and C for each reaction is defined as

$$P(E_a, C|\{R_{TST}, \sigma\}) = \prod_{i=1}^{N_k} P[E_a, C|R_{TST}(T_i), \sigma_i]$$
$$= \prod_{i=1}^{N_k} \frac{1}{\sqrt{2\pi\sigma_i^2}} \exp\left\{-\frac{[R_{TST}(T_i) - R(C, E_a, T_i)]^2}{2\sigma_i^2}\right\} \tag{17}$$

where N_k is the number of reaction rates calculated using transition state theory, $R_{TST}(T_i)$ is the TST reaction rate calculated at temperature T_i, and σ_i is the uncertainty in the corresponding TST reaction rate. The likelihood distributions of these parameters for Langmuir−Hinshelwood recombination and thermal desorption in strong surface sites can be seen in

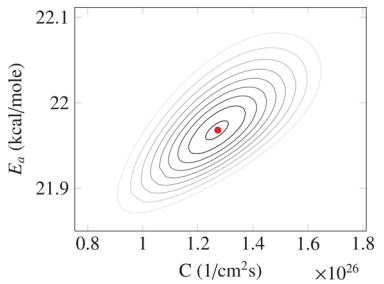

Figure 13. Likelihood of activation energy (E_a) and pre-exponential factor (C) for LH recombination in strong surface sites. The maximum likelihood point is marked by a red dot.

Figures 13 and 14, respectively. The maximum likelihood points and the errors we obtained from the least-squares fits are

$$E_a = 21.96 \pm 0.1 \text{ kcal/mol}$$
$$C = (1.28 \pm 0.2) \times 10^{26}\ 1/(\text{cm}^2\,\text{s})$$

DOI: 10.1021/acs.jpcc.6b07365
J. Phys. Chem. C 2016, 120, 24137−24147

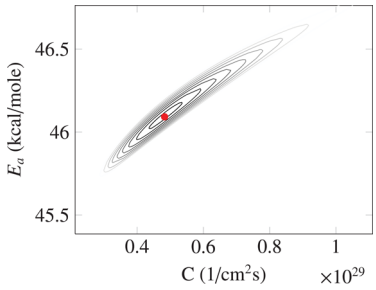

Figure 14. Likelihood of activation energy (E_a) and pre-exponential factor (C) for thermal desorption in strong surface sites. The maximum likelihood point is marked by a red dot.

for LH recombination of hydrogen in the strongly bound state and

$$E_a = 46.06 \pm 0.2 \text{ kcal/mol}$$
$$C = (4.6 \pm 2) \times 10^{28} \text{ 1/(cm}^2 \text{ s)}$$

for thermal desorption of hydrogen in the strongly bound state. For hydrogen in weak surface sites, we found

$$E_a = 1.22 \pm 0.02 \text{ kcal/mol}$$
$$C = (3.4 \pm 0.6) \times 10^{26} \text{ 1/(cm}^2 \text{ s)}$$

for LH recombination and

$$E_a = 2.18 \pm 0.02 \text{ kcal/mol}$$
$$C = (2.5 \pm 0.5) \times 10^{27} \text{ 1/(cm}^2 \text{ s)}$$

for thermal desorption.

The activation energies here compare well to values estimated in other studies (see Table 2). The activation energies calculated for reactions in strong surface sites are closest to those of Wood and Wise,[30] whereas values for reactions in weak sites show better agreement with energies predicted by Gelb and Kim.[26] However, it should be noted that the latter model does not account for Langmuir−Hinshelwood recombination. Because the activation energy for thermal desorption of the weakly bound state is higher than that predicted by Wood and Wise,[30] hydrogen atoms linger in weak surface sites at higher temperatures. Recombination of weakly bound hydrogen remaining on the surface leads to higher recombination coefficients in the low-temperature regime, as can be seen in Figure 15.

Table 2. Activation Energies for Reactions of Strongly Bound (S) and Weakly Bound (W) Hydrogen on Silica Predicted by Various Surface Chemistry Models

	activation energy (kcal/mol)		
reaction	Wood/Wise[30]	Gelb/Kim[26]	this work
LH recombination (S)	22.5	–	21.96
atomic desorption (S)	45	42	46.06
LH recombination (W)	0.75	–	1.22
atomic desorption (W)	1.5	2.1	2.18

3. DISCUSSION

3.1. Langmuir Kinetics Model. After calculating Eley−Rideal, Langmuir−Hinshelwood, and thermal desorption rates for hydrogen atoms in strong and weak binding sites, we calculated steady-state coverage of these sites by finding the fractional coverage that satisfied a simple Langmuir kinetics model. Steady-state coverage for sites of type i is defined as the fractional coverage θ_i that satisfies the equation

$$\underbrace{(1-\theta_i)k_A}_{\text{adsorption rate}} = \underbrace{2\theta_i^2 R_{LH,i}}_{\text{LH desorption}} + \underbrace{\theta_i R_{ER,i}}_{\text{ER desorption}} + \underbrace{\theta_i R_{d,i}}_{\text{thermal desorption}} \quad (18)$$

where k_a is the rate at which H radicals impinge on the surface assuming a sticking coefficient of unity, given by

$$k_A = n_H \left(\frac{k_B T}{2\pi m_H}\right)^{1/2} \quad (19)$$

Once we had found the steady-state coverage for the temperature and gas-phase radical density of interest, we calculated a recombination coefficient based on the ratio of the reactive flux to the incident flux of radicals

$$\gamma = \frac{2\Gamma_{H_2,out}}{\Gamma_{H,in}} = \frac{2(\theta_S^2 R_{LH,S} + \theta_S R_{ER,S} + \theta_W^2 R_{LH,W} + \theta_W R_{ER,W})}{k_A} \quad (20)$$

where the subscripts S and W denote the reaction rates and coverages of strong and weak surface sites, respectively.

A comparison between molecular dynamics results and a Langmuir kinetics model paramterized using our Monte Carlo procedure can be seen in Figure 3. In this high-pressure extreme, the model is able to reproduce the behavior seen in MD simulations, although the molecular dynamics data generally fall above model predictions. This may be the result of multilayer coverage of physisorbed hydrogen atoms, particularly in the low-temperature limit. Any additional atoms sticking to the surface would increase the effective number of surface sites for recombination and be even more weakly bound than atoms in the first physisorbed layer.

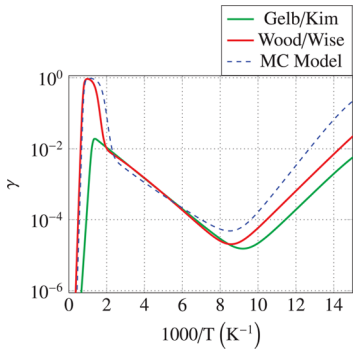

Figure 15. Comparison of the recombination coefficient calculated with Monte Carlo results to Langmuir kinetics models from the literature.

3.2. Comparison to Other Models. Few detailed studies of the behavior of H recombination on silica exist in the literature, and the recombination coefficients predicted by the available models vary greatly. Although the recombination coefficient estimated by our model shows the same temperature dependence as those predicted by the models of Wood and Wise[30] and Gelb and Kim,[26] it is significantly higher than the values proposed by Kim and Boudart[21] at high temperatures. As

DOI: 10.1021/acs.jpcc.6b07365
J. Phys. Chem. C 2016, 120, 24137−24147

can be seen in Figure 15 for $n_H = 10^{12}$ cm^{-3}, the Langmuir kinetics model parametrized with Monte Carlo simulations displays the complex, non-Arrhenius behavior found in previous experimental studies. This model predicts a maximum of the recombination coefficient between 500 and 2000 K due to Langmuir−Hinshelwood recombination and reliably produces a recombination coefficient within an order of magnitude of that predicted by the model of Wood and Wise.[30]

Several experimental studies have also estimated the recombination coefficient at 300 K using a variety of techniques, including the planar laser-induced fluorescence (PLIF) and laser-induced fluorescence (LIF) methods. The recombination coefficient at a gas-phase number density of 10^{16} cm^{-3} and 300 K also agrees with the results of these experiments (see Table 3). As this Monte Carlo procedure does not take into account the "poisoning" of surface reactions due to adsorbed molecular species blocking active sites on the surface, the calculated recombination coefficient represents an upper bound. Recombination in physisorption sites is particularly susceptible to poisoning, one possible explanation for this model's overprediction of γ at low temperatures when compared to models that have been calibrated with experimental data. Because of the high heat of physisorption of water on quartz (10−20 kcal/mol[55,56]), H_2O is a powerful inhibitor of the surface reactions investigated here. In experiments described in ref 57, the addition of water vapor to hydrogen plasma increased the gas-phase concentration of atomic hydrogen by a factor of 90, as a result of suppressed recombination on the quartz walls of the reaction vessel.

Table 3. Experimental Estimates of the Recombination Coefficient for H on Silica at T_{surf} = 300 K

source	γ(300 K)	n_H (cm^{-3})
ref 58	2.22×10^{-3}	10^{16}
ref 59	$>10^{-3}$	10^{12} [a]
ref 60	1.8×10^{-5}	10^{16} [a]
this work	1.9×10^{-3}	10^{16}

[a] n_H estimated based on pressure and a dissociation degree of 0.1.

The roughness of the quartz surface should also be considered in comparisons with models calibrated with experimental data. As investigated by Kim and Boudart[21] with silica powder on quartz surfaces, recombination rates increase linearly with microscale surface roughness.[21] Even atomic-scale surface roughness can increase the density of defects and adsorption sites, thereby increasing reaction rates.

4. CONCLUSIONS

The recombination rates of hydrogen have been evaluated on clean surfaces using atomic-scale calculations to quantify reaction rates and build a multi-time-scale Langmuir kinetics model for hydrogen recombination.

Molecular dynamics simulations were used to measure recombination coefficients in a high-pressure regime inaccessible to experiments, providing additional data against which to compare model predictions. MD simulations were carried out for temperatures between 10 and 600 K at a gas-phase radical number density of 2.7×10^{20} cm^{-3}. The recombination coefficient was high under these conditions, never dropping far below 0.1 for the simulated temperatures and reaching a maximum at about 275 K.

The Eley−Rideal, Langmuir−Hinshelwood, and thermal desorption mechanisms were considered as part of the Langmuir kinetics model for hydrogen recombination. Values of rate constants in this model were found using grand canonical Monte Carlo and Monte Carlo variational transition state theory calculations. GCMC simulations provided the densities and strengths of adsorption sites on the silica surface. Strong and weak binding sites for hydrogen on a silica surface are found, with densities of 9.3 and 10.5 nm^{-2}, respectively. Using semiequilibrium theory with the heat of adsorption for hydrogen atoms, an Eley−Rideal rate constant was calculated.

The rates of the Langmuir−Hinshelwood and thermal desorption reactions were quantified using MCVTST calculations. The collected reaction rates were found to follow an Arrhenius trend. Activation energies and pre-exponential factors were estimated using a least-squares fit, and the activation energy for desorption was found to be approximately twice that for Langmuir−Hinshelwood recombination, although the greater pre-exponential factor for desorption indicates that it dominates at high temperatures. The activation energies for recombination and desorption agree with existing models, particularly those predicted by Gelb and Kim.[26]

The Langmuir kinetics model with TST reaction rates was found to be capable of reproducing the non-Arrhenius behavior of the recombination coefficient seen in both the high-pressure molecular dynamics simulations and low-pressure experiments. The estimated recombination rates were significantly higher than those obtained by the Kim and Boudart[21] model, whereas quantitative agreement was achieved with the more reactive surface model of Wood and Wise.[30] The predicted recombination coefficient was greater than those obtained using experimentally calibrated models at low temperatures, possibly as a result of surface poisoning due to adsorbed molecules.

The Arrhenius parameters found in this work are intended for use in a surface chemistry model for continuum-scale combustion simulations to account for radical quenching near walls. The combined effects of heat generation and radical destruction due to surface reactions have been shown to influence flame ignition and extinction; quantifying these reaction rates is important for the predictive simulation and design of combustion devices, particularly those with high surface-to-volume ratios.

Finally, we note that the methods used here are not restricted to the study of hydrogen on silica. A similar Monte Carlo procedure can be used to calculate recombination rates on any surface where the Eley−Rideal and Langmuir−Hinshelwood mechanisms are prevalent.

AUTHOR INFORMATION

Corresponding Author

*E-mail: htj@illinois.edu. Phone: 217-265-5468.

Notes

The authors declare no competing financial interest.

ACKNOWLEDGMENTS

This material is based in part on work supported by the National Nuclear Security Administration, U.S. Department of Energy, under Award DE-NA0002374.

REFERENCES

(1) Biham, O.; Furman, I.; Pirronello, V.; Vidali, G. Master Equation for Hydrogen Recombination on Grain Surfaces. *Astrophys. J.* **2001**, *553*, 595.

DOI: 10.1021/acs.jpcc.6b07365
J. Phys. Chem. C 2016, 120, 24137−24147

(2) Biham, O.; Lipshtat, A. Exact Results for Hydrogen Recombination on Dust Grain Surfaces. *Phys. Rev. E: Stat. Phys., Plasmas, Fluids, Relat. Interdiscip. Top.* **2002**, *66*, 056103.
(3) Cazaux, S.; Tielens, A. Molecular Hydrogen Formation in the Interstellar Medium. *Astrophys. J.* **2002**, *575*, L29.
(4) Cazaux, S.; Caselli, P.; Tielens, A. G. G. M.; Le Bourlot, J.; Walmsley, M. Molecular Hydrogen Formation on Grain Surfaces. *J. Phys.: Conf. Ser.* **2005**, *6*, 155.
(5) Zecho, T.; Güttler, A.; Sha, X.; Jackson, B.; Küppers, J. Adsorption of Hydrogen and Deuterium Atoms on the (0001) Graphite Surface. *J. Chem. Phys.* **2002**, *117*, 8486−8492.
(6) Ferro, Y.; Marinelli, F.; Allouche, A. Density Functional Theory Investigation of the Diffusion and Recombination of H on a Graphite Surface. *Chem. Phys. Lett.* **2003**, *368*, 609−615.
(7) Ferro, Y.; Marinelli, F.; Allouche, A. Density Functional Theory Investigation of H Adsorption and H_2 Recombination on the Basal Plane and in the Bulk of Graphite: Connection Between Slab and Cluster Model. *J. Chem. Phys.* **2002**, *116*, 8124−8131.
(8) Züttel, A.; Orimo, S.-i. Hydrogen in Nanostructured, Carbon-Related, and Metallic Materials. *MRS Bull.* **2002**, *27*, 705−711.
(9) Cheng, J.; Yuan, X.; Zhao, L.; Huang, D.; Zhao, M.; Dai, L.; Ding, R. GCMC Simulation of Hydrogen Physisorption on Carbon Nanotubes and Nanotube Arrays. *Carbon* **2004**, *42*, 2019−2024.
(10) Hickmott, T. Interaction of Atomic Hydrogen with Glass. *J. Appl. Phys.* **1960**, *31*, 128−136.
(11) St-Onge, L.; Moisan, M. Hydrogen Atom Yield in RF and Microwave Hydrogen Discharges. *Plasma Chem. Plasma Process.* **1994**, *14*, 87−116.
(12) Zyryanov, S.; Kovalev, A.; Lopaev, D.; Malykhin, E.; Rakhimov, A.; Rakhimova, T.; Koshelev, K.; Krivtsun, V. Loss of Hydrogen Atoms in H2 Plasma on the Surfaces of Materials Used in EUV Lithography. *Plasma Phys. Rep.* **2011**, *37*, 881−889.
(13) Pfefferle, L.; Pfefferle, W. Catalysis in Combustion. *Catal. Rev.: Sci. Eng.* **1987**, *29*, 219−267.
(14) Prakash, S.; Akberov, R.; Agonafer, D.; Armijo, A. D.; Shannon, M. A. Influence of Boundary Conditions on Sub-Millimeter Combustion. *Energy Fuels* **2009**, *23*, 3549−3557.
(15) Prakash, S.; Glumac, N. G.; Shankar, N.; Shannon, M. A. OH Concentration Profiles over Alumina, Quartz, and Platinum Surfaces using Laser-Induced Fluorescence Spectroscopy in Low-Pressure Hydrogen/Oxygen Flames. *Combust. Sci. Technol.* **2005**, *177*, 793−817.
(16) Kim, K. T.; Lee, D. H.; Kwon, S. Effects of Thermal and Chemical Surface−Flame Interaction on Flame Quenching. *Combust. Flame* **2006**, *146*, 19−28.
(17) Chen, G.-B.; Chen, C.-P.; Wu, C.-Y.; Chao, Y.-C. Effects of Catalytic Walls on Hydrogen/Air Combustion Inside a Micro-Tube. *Appl. Catal., A* **2007**, *332*, 89−97.
(18) Langmuir, I. The Dissociation of Hydrogen Into Atoms. III. The Mechanism of the Reaction. *J. Am. Chem. Soc.* **1916**, *38*, 1145−1156.
(19) Langmuir, I. The Adsorption of Gases on Plane Surfaces of Glass, Mica and Platinum. *J. Am. Chem. Soc.* **1918**, *40*, 1361−1403.
(20) Johnson, M. The Adsorption of Hydrogen on the Surface of an Electrodeless Discharge Tube. *Proc. R. Soc. London, Ser. A* **1929**, *123*, 603−613.
(21) Kim, Y. C.; Boudart, M. Recombination of Oxygen, Nitrogen, and Hydrogen Atoms on Silica: Kinetics and Mechanism. *Langmuir* **1991**, *7*, 2999−3005.
(22) Wood, B. J.; Wise, H. The Kinetics of Hydrogen Atom Recombination on Pyrex Glass and Fused Quartz. *J. Phys. Chem.* **1962**, *66*, 1049−1053.
(23) Frennet, A.; Wells, P. B. Characterization of the Standard Platinum/Silica Catalyst EUROPT-1. 4. Chemisorption of Hydrogen. *Appl. Catal.* **1985**, *18*, 243−257.
(24) De Boer, J. H. Heterogeneous Catalysis and the Strength of the Chemisorptive Bonds. *Bull. Soc. Chim. Belg.* **1958**, *67*, 284−304.
(25) Hollenbach, D.; Thronson, H. *Interstellar Processes*, 1st ed.; Springer: Dordrecht, The Netherlands, 1987.
(26) Gelb, A.; Kim, S. K. Theory of Atomic Recombination on Surfaces. *J. Chem. Phys.* **1971**, *55*, 4935−4939.
(27) Cozmuta, I. Molecular Mechanisms of Gas Surface Interactions in Hypersonic Flow. In *Proceedings of the 39th AIAA Thermophysics Conference*; American Institute of Aeronautics and Astronautics (AIAA): Reston, VA, 2007; AIAA 2007-4046.
(28) Norman, P.; Schwarztentruber, T.; Cozmuta, I. Modeling Air-SiO_2 Surface Catalysis under Hypersonic Conditions with ReaxFF Molecular Dynamics. In *Proceedings of the 10th AIAA/ASME Joint Thermophysics and Heat Transfer Conference*; American Institute of Aeronautics and Astronautics (AIAA): Reston, VA, 2010; AIAA 2010-4320.
(29) Rutigliano, M.; Gamallo, P.; Sayós, R.; Orlandini, S.; Cacciatore, M. A Molecular Dynamics Simulation of Hydrogen Atoms Collisions on an H-Preadsorbed Silica Surface. *Plasma Sources Sci. Technol.* **2014**, *23*, 045016.
(30) Wood, B. J.; Wise, H. Kinetics of Hydrogen Atom Recombination on Surfaces. *J. Phys. Chem.* **1961**, *65*, 1976−1983.
(31) Smith, W. The Surface Recombination of H Atoms and OH Radicals. *J. Chem. Phys.* **1943**, *11*, 110−125.
(32) Plimpton, S. Fast Parallel Algorithms for Short-Range Molecular Dynamics. *J. Comput. Phys.* **1995**, *117*, 1−19.
(33) van Duin, A. C.; Strachan, A.; Stewman, S.; Zhang, Q.; Xu, X.; Goddard, W. A. $ReaxFF_{SiO}$ Reactive Force Field for Silicon and Silicon Oxide Systems. *J. Phys. Chem. A* **2003**, *107*, 3803−3811.
(34) Khalilov, U.; Neyts, E.; Pourtois, G.; van Duin, A. C. Can We Control the Thickness of Ultrathin Silica Layers by Hyperthermal Silicon Oxidation at Room Temperature? *J. Phys. Chem. C* **2011**, *115*, 24839−24848.
(35) Buehler, M. J.; van Duin, A. C.; Goddard, W. A., III. Multiparadigm Modeling of Dynamical Crack Propagation in Silicon Using a Reactive Force Field. *Phys. Rev. Lett.* **2006**, *96*, 095505.
(36) Yeon, J.; van Duin, A. C. ReaxFF Molecular Dynamics Simulations of Hydroxylation Kinetics for Amorphous and Nano-Silica Structure, and Its Relations with Atomic Strain Energy. *J. Phys. Chem. C* **2016**, *120*, 305−317.
(37) Yue, D.-C.; Ma, T.-B.; Hu, Y.-Z.; Yeon, J.; van Duin, A. C.; Wang, H.; Luo, J. Tribochemistry of Phosphoric Acid Sheared Between Quartz Surfaces: A Reactive Molecular Dynamics Study. *J. Phys. Chem. C* **2013**, *117*, 25604−25614.
(38) Van Duin, A. C.; Dasgupta, S.; Lorant, F.; Goddard, W. A. ReaxFF: A Reactive Force Field for Hydrocarbons. *J. Phys. Chem. A* **2001**, *105*, 9396−9409.
(39) Norman, P.; Schwartzentruber, T. E.; Leverentz, H.; Luo, S.; Meana-Paneda, R.; Paukku, Y.; Truhlar, D. G. The Structure of Silica Surfaces Exposed to Atomic Oxygen. *J. Phys. Chem. C* **2013**, *117*, 9311−9321.
(40) Fogarty, J. C.; Aktulga, H. M.; Grama, A. Y.; Van Duin, A. C.; Pandit, S. A. A Reactive Molecular Dynamics Simulation of the Silica-Water Interface. *J. Chem. Phys.* **2010**, *132*, 174704.
(41) Frenkel, D.; Smit, B. *Understanding Molecular Simulation: From Algorithms to Applications*, 2nd ed.; Academic Press: San Diego, 2002.
(42) Valentini, P.; Schwartzentruber, T. E.; Cozmuta, I. ReaxFF Grand Canonical Monte Carlo Simulation of Adsorption and Dissociation of Oxygen on Platinum (111). *Surf. Sci.* **2011**, *605*, 1941−1950.
(43) Presber, M.; Dünweg, B.; Landau, D. Monte Carlo Studies of Adsorbed Monolayers: Lattice-Gas Models With Translational Degrees of Freedom. *Phys. Rev. E: Stat. Phys., Plasmas, Fluids, Relat. Interdiscip. Top.* **1998**, *58*, 2616.
(44) Meana-Paneda, R.; Paukku, Y.; Duanmu, K.; Norman, P.; Schwartzentruber, T. E.; Truhlar, D. G. Atomic Oxygen Recombination at Surface Defects on Reconstructed (0001) α-Quartz Exposed to Atomic and Molecular Oxygen. *J. Phys. Chem. C* **2015**, *119*, 9287−9301.
(45) Johnson, M. Pressure Measurements for Investigating the Mutual Behaviour of Adsorbed Hydrogen Atoms. *Trans. Faraday Soc.* **1932**, *28*, 162−165.

DOI: 10.1021/acs.jpcc.6b07365
J. Phys. Chem. C 2016, 120, 24137−24147

(46) Langmuir, I. A Chemically Active Modification of Hydrogen. *J. Am. Chem. Soc.* **1912**, *34*, 1310−1325.
(47) Zhuravlev, L. The Surface Chemistry of Amorphous Silica. Zhuravlev Model. *Colloids Surf., A* **2000**, *173*, 1−38.
(48) NoorBatcha, I.; Raff, L. M.; Thompson, D. L. Monte Carlo Random Walk Study of Recombination and Desorption of Hydrogen on Si (111). *J. Chem. Phys.* **1985**, *83*, 1382−1391.
(49) Raff, L. M.; NoorBatcha, I.; Thompson, D. L. Monte Carlo Variational Transition-State Theory Study of Recombination and Desorption of Hydrogen on Si (111). *J. Chem. Phys.* **1986**, *85*, 3081−3089.
(50) Agrawal, P. M.; Rice, B. M.; Thompson, D. L. Predicting Trends in Rate Parameters for Self-Diffusion on FCC Metal Surfaces. *Surf. Sci.* **2002**, *515*, 21−35.
(51) Shalashilin, D. V.; Thompson, D. L. Monte Carlo Variational Transition-State Theory Study of the Unimolecular Dissociation of RDX. *J. Phys. Chem. A* **1997**, *101*, 961−966.
(52) Doll, J. A Unified Theory of Dissociation. *J. Chem. Phys.* **1980**, *73*, 2760−2762.
(53) Doll, J. Monte Carlo Sampling Techniques and the Evaluation of Unimolecular Rate Constants. *J. Chem. Phys.* **1981**, *74*, 1074−1077.
(54) Shalashilin, D. V.; Thompson, D. L. Intrinsic Non-RRK Behavior: Classical Trajectory, Statistical Theory, and Diffusional Theory Studies of a Unimolecular Reaction. *J. Chem. Phys.* **1996**, *105*, 1833−1845.
(55) Hackerman, N.; Hall, A. C. The Adsorption of Water Vapor on Quartz and Calcite. *J. Phys. Chem.* **1958**, *62*, 1212−1214.
(56) Whalen, J. Thermodynamic Properties of Water Adsorbed on Quartz. *J. Phys. Chem.* **1961**, *65*, 1676−1681.
(57) Kikuchi, J.; Suzuki, M.; Yano, H.; Fujimura, S. Effects of H_2O on Atomic Hydrogen Generation in Hydrogen Plasma. *Proc. SPIE* **1992**, *1803*, 70−76.
(58) Tomasini, L.; Rousseau, A.; Baravian, G.; Gousset, G.; Leprince, P. Laser Induced Stimulated Emission for Hydrogen Atom Density Measurements in a Hydrogen Pulsed Microwave Discharge. *Appl. Phys. Lett.* **1996**, *69*, 1553−1555.
(59) Sheen, D. B. Adsorption and Recombination of Hydrogen Atoms on Glass Surfaces. Part 1. Method of Study and the Mechanism of Recombination at 77 and 273 K. *J. Chem. Soc., Faraday Trans. 1* **1979**, *75*, 2439−2453.
(60) Sancier, K. M.; Wise, H. Diffusion and Heterogeneous Reaction. XI. Diffusion Coefficient Measurements for Gas Mixture of Atomic and Molecular Hydrogen. *J. Chem. Phys.* **1969**, *51*, 1434−1438.

DOI: 10.1021/acs.jpcc.6b07365
J. Phys. Chem. C 2016, 120, 24137−24147